A&A 479, 493–501 (2008)
DOI: 10.1051/0004-6361:20078956

Astronomy & Astrophysics

Detection of circumstellar CH_2CHCN, CH_2CN, CH_3CCH, and H_2CS⋆

M. Agúndez[1], J. P. Fonfría[1], J. Cernicharo[1], J. R. Pardo[1], and M. Guélin[2]

[1] Departamento de Astrofísica Molecular e Infrarroja, Instituto de Estructura de la Materia, CSIC, Serrano 121, 28006 Madrid, Spain
e-mail: [marce;pablo;cerni;pardo]@damir.iem.csic.es
[2] Institut de Radioastronomie Millimétrique, 300 rue de la Piscine, 38406 St. Martin d'Hères and LERMA/École Normale Supérieure, 24 rue Lhomond, 75231 Paris, France
e-mail: guelin@iram.fr

Received 29 October 2007 / Accepted 6 December 2007

ABSTRACT

Aims. We report on the detection of vinyl cyanide (CH_2CHCN), cyanomethyl radical (CH_2CN), methylacetylene (CH_3CCH), and thioformaldehyde (H_2CS) in the C-rich star IRC +10216. These species, which are all known to exist in dark clouds, were detected for the first time in the circumstellar envelope around an AGB star.
Methods. The four molecules were detected through pure rotational transitions in the course of a λ 3 mm line survey carried out with the IRAM 30-m telescope. The molecular column densities were derived by constructing rotational temperature diagrams. A detailed chemical model of the circumstellar envelope is used to analyze the formation of these molecular species.
Results. We have found column densities in the range 5×10^{12}–2×10^{13} cm^{-2}, which translates to fractional abundances relative to H_2 of several 10^{-9}. The chemical model is reasonably successful in explaining the derived abundances through gas phase synthesis in the cold outer envelope. We also find that some of these molecules, CH_2CHCN and CH_2CN, are most probably excited through infrared pumping to excited vibrational states.
Conclusions. The detection of these species stresses the similarity between the molecular content of cold dark clouds and C-rich circumstellar envelopes. However, some differences in the chemistry are indicated by partially saturated carbon chains being present in IRC +10216 at a lower level than those that are highly unsaturated, while in TMC-1 both types of species have comparable abundances.

Key words. astrochemistry – stars: circumstellar matter – stars: AGB and post-AGB – stars: carbon – stars: individual: IRC +10216

1. Introduction

The chemical complexity of circumstellar envelopes (CSEs) around carbon-rich AGB stars is illustrated by the well known object IRC +10216, where more than 60 different molecular species have been identified to date. Due to the carbon-rich nature of the gas, the vast majority are oxygen-deprived hydrocarbons with a very concrete structure consisting of a linear and highly unsaturated backbone of carbon atoms. Among these species are cyanopolyynes $HC_{2n+1}N$, polyacetylenic radicals C_nH, carbenes H_2C_n, allenic radicals $HC_{2n}N$, as well as sulphur and silicon-bearing carbon chains C_nS, SiC_n (Cernicharo et al. 2000). The synthesis of these molecules involves the photodissociation and photoionisation by interstellar UV photons of parent species out-flowing from the star and subsequent neutral-neutral and ion-molecule gas phase reactions in the cold outer envelope (e.g. Lafont et al. 1982; Nejad & Millar 1987; Millar & Herbst 1994; Millar et al. 2000). Thus, reactive molecules are distributed in circumstellar shells, as confirmed by interferometric observations (e.g. Guélin et al. 1993).

This type of chemistry resembles what is occurring in cold dense clouds, such as TMC-1, which are also rich in highly unsaturated carbon chain molecules. The unsaturated character is typically the result of low temperature non-equilibrium chemistry and reflects the low reactivity of H_2 with most hydrocarbons at low temperatures. Dark clouds contain however a sizable fraction of partially saturated species, such as methylpolyynes $CH_3C_{2n}H$ ($n = 1, 2$ Irvine et al. 1981; Walmsley et al. 1984), methylcyanopolyynes $CH_3C_{2n+1}N$ ($n = 0, 1, 2$ Matthews & Sears 1983a; Broten et al. 1984; Snyder et al. 2006), cyanomethyl radical CH_2CN (Irvine et al. 1988), vinyl cyanide CH_2CHCN (Matthews & Sears 1983b), cyanoallene CH_2CCHCN (Lovas et al. 2006), and highly saturated hydrocarbons such as propylene CH_2CHCH_3 (Marcelino et al. 2007).

The question of why those partially saturated species are not detected in IRC +10216 is a critical one for the understanding of low-temperature non-equilibrium chemistry. We have thus embarked on a deep search for partially saturated organic molecules in IRC +10216. In this paper we present the detection of CH_2CHCN, CH_2CN and CH_3CCH, which were observed for the first time in a CSE around an AGB star. The related species CH_3CN has been already identified in this source by Johansson et al. (1984). Finally, we also report on the detection of thioformaldehyde in IRC +10216.

2. Spectroscopy and observations

The four molecules in this paper (CH_2CHCN, CH_2CN, CH_3CCH, and H_2CS) were identified in space for the first time towards Sagittarius B2 (Gardner & Winnewisser 1975; Irvine et al. 1988; Snyder & Buhl 1973; Sinclair et al. 1973) by

⋆ Based on observations carried out with the IRAM 30-m telescope. IRAM is supported by INSU/CNRS (France), MPG (Germany) and IGN (Spain).

observation of rotational transitions. The microwave spectrum of all these species has been extensively studied in the laboratory so that their spectroscopic properties are accurately known; see a compilation in the JPL and Cologne databases for molecular spectroscopy (Pickett et al. 1998; Müller et al. 2005).

CH_2CHCN is a planar asymmetric rotor with a- and b-type allowed transitions (μ_a = 3.815 D and μ_b = 0.894 D; Stolze & Sutter 1985). All the transitions observed in IRC +10216 belong to the stronger a-type.

The radical CH_2CN has two interchangeable hydrogen nuclei with non zero spin which result in two distinct groups of rotational levels: ortho (parallel spins) and para (antiparallel spins) with relative statistical weights 3:1, between which both radiative and collisional transitions are highly forbidden. The electronic ground state is $^2B_1$, thus, the quantum number K_a is even for ortho levels and odd for para levels. The para ground state ($1_{1,1}$) lies 14.15 K above the ortho ground state ($0_{0,0}$). This assignment is reversed compared to more common species with a $^1A_1$ electronic ground state (H_2CO, H_2CS, ...), where the quantum number K_a is odd for ortho levels and even for para levels, with the rotational ground state having para symmetry. Its dipole moment is relatively large: μ_a = 3.5 D (Ozeki et al. 2004). The unpaired electron causes spin-rotation coupling which splits each transition $N'_{K'_a,K'_c}$-$N''_{K''_a,K''_c}$ into two components. Further hyperfine coupling of rotation with the non-zero spin of ^{1}H and ^{14}N nuclei produces a myriad of components whose frequencies have been precisely measured in the laboratory (Ozeki et al. 2004).

Propyne (CH_3CCH) is a prolate symmetric top molecule whose rotational levels are divided into two different species, A-type and E-type, not connected radiatively. Its dipole moment is relatively small: μ_a = 0.784 D (Burrell et al. 1980). The rotational spectrum was first measured by Trambarulo & Gordy (1950) and is now known with a high accuracy for its ground and some excited vibrational states (Müller et al. 2002).

H_2CS is an asymmetric rotor which, analogously to CH_2CN, has two interchangeable hydrogen nuclei so that its rotational levels are grouped into ortho (K_a odd) and para (K_a even), with statistical weights 3:1. The ortho ground state ($1_{1,1}$) lies 14.9 K above the para ground state ($0_{0,0}$). Its dipole moment was measured by Fabricant et al. (1977) to be μ_a = 1.647 D.

The observations shown in Fig. 1 were made with the IRAM 30-m telescope during several sessions from 1990 to 2006, most of them after 2002 in the context of a λ 3 mm line survey of IRC +10216 (Cernicharo et al., in preparation). SIS receivers operating at 3 and 2 mm were tuned in single sideband mode, with typical image rejections larger than 20 dB at 3 mm and around 15 dB at 2 mm. We express intensities in terms of T_A^*, the antenna temperature corrected for atmospheric absorption and for antenna ohmic and spillover losses. The uncertainty in T_A^* due to calibration is estimated to be around 10%. Data were taken in the standard wobbler switching mode with a beam throw of 4′. Pointing and focusing were checked by observing nearby planets and the quasar OJ 287. The back end used was a filterbank with a bandwidth of 512 MHz and a spectral resolution of 1.0 MHz. The system temperature was 100−150 K at 3 mm and 200 K at 2 mm. On source integration times ranged from 2 to 20 h, resulting in rms noise levels of 1−3 mK in T_A^*.

3. Results

Figure 1 shows the observed spectra of IRC +10216 corresponding to the CH_2CHCN, CH_2CN, CH_3CCH, and H_2CS lines. The observational line parameters, obtained by using the SHELL fitting routine of the CLASS package[1], are given in Table 1. Linewidths have been fixed in many cases due to limited signal-to-noise (S/N) ratio or due to blending with other lines. The measured widths are consistent with an expansion velocity v_{exp} around 14.5 km s^{-1}, in agreement with most of the molecular lines arising from the expanding envelope of IRC +10216 (Cernicharo et al. 2000). There are no missing lines of CH_2CN, CH_3CCH or H_2CS in the 3 mm atmospheric window. However, some lines of CH_2CHCN having similar strengths and upper level energies to those reported in Table 1 are not listed due to a complete blending with a stronger line or due to a low sensitivity of the spectra. For example the $11_{0,11}$−$10_{0,10}$ transition at 103 575 MHz is blended with a strong component of the J = 21/2−19/2 $^2\Pi_{1/2}$ v_7 = 1 doublet of C_4H.

The line profiles can give us information on the spatial distribution of the molecules. In a spherically expanding envelope and for lines with a low optical depth, a double-peaked shape indicates that the emitting species has a distribution with an angular extent comparable or larger than the telescope beam ($HPBW$ = 21″−31″ for IRAM 30-m at λ 3 mm), while a flat-topped profile indicates that the emitting region is not spatially resolved by the telescope beam. The lines of CH_3CN in IRC +10216 have a double-peaked character (see Fig. 1), which indicates that this molecule has an extended distribution. In the case of the four species with which we are concerned, the low S/N ratio of most of the observed lines makes it difficult to distinguish whether line profiles are predominantly double-peaked or flat-topped for a given species. Therefore, any conclusion about the spatial distribution of the molecules derived from the line profiles must be taken with caution. We will, nevertheless, consider that CH_2CHCN, CH_2CN, CH_3CCH, and H_2CS have an extended distribution, based on chemical arguments (see Sect. 3.2 and Fig. 3), which essentially fills the telescope beam. Under such hypothesis, we have constructed rotational temperature diagrams to derive beam averaged column densities.

For CH_2CHCN (see Fig. 2) we derive a total column density N_{tot} = (5.5 ± 1.5) × 10^{12} cm^{-2} and a rotational temperature of 46 ± 16 K, which is within the range of rotational temperatures derived for other shell-distributed molecules in IRC +10216: 20−50 K (Cernicharo et al. 2000).

In the case of CH_2CN, we have used all the observed lines – ortho and para – in a single rotational diagram (see Fig. 2). Given that the lines are detected with a low S/N ratio, we do not aim at determining the O/P ratio although the available data is consistent with the statistical value 3:1. We derive a rotational temperature of 50 ± 13 K and a total column density of N_{tot} = (8.6 ± 1.4) × 10^{12} cm^{-2}, which is comparable to that of the related species CH_3CN (see Table 2).

The two CH_3CCH lines detected are very likely a sum of the K = 0, 1 components, although the low S/N ratio does not allow us to clearly distinguish them. Assuming a rotational temperature of 30 K we tentatively derive a total column density of 1.8 × 10^{13} cm^{-2}. This value is comparable to the column density of CH_3CN in IRC +10216, which is detected through lines about 25 times stronger than those of CH_3CCH due to its much larger dipole moment (μ_{CH_3CN} = 3.925 D versus μ_{CH_3CCH} = 0.780 D).

Both CH_3CN and CH_3CCH have been also detected in the C-rich preplanetary nebula CRL 618 (Cernicharo et al. 2001; Pardo & Cernicharo 2006; Pardo et al. 2007; see also Fig. 1), which is in a evolutionary stage immediately following that of IRC +10216. However, the CH_3CCH/CH_3CN ratio is noticeably

[1] http://www.iram.fr/IRAMFR/GILDAS

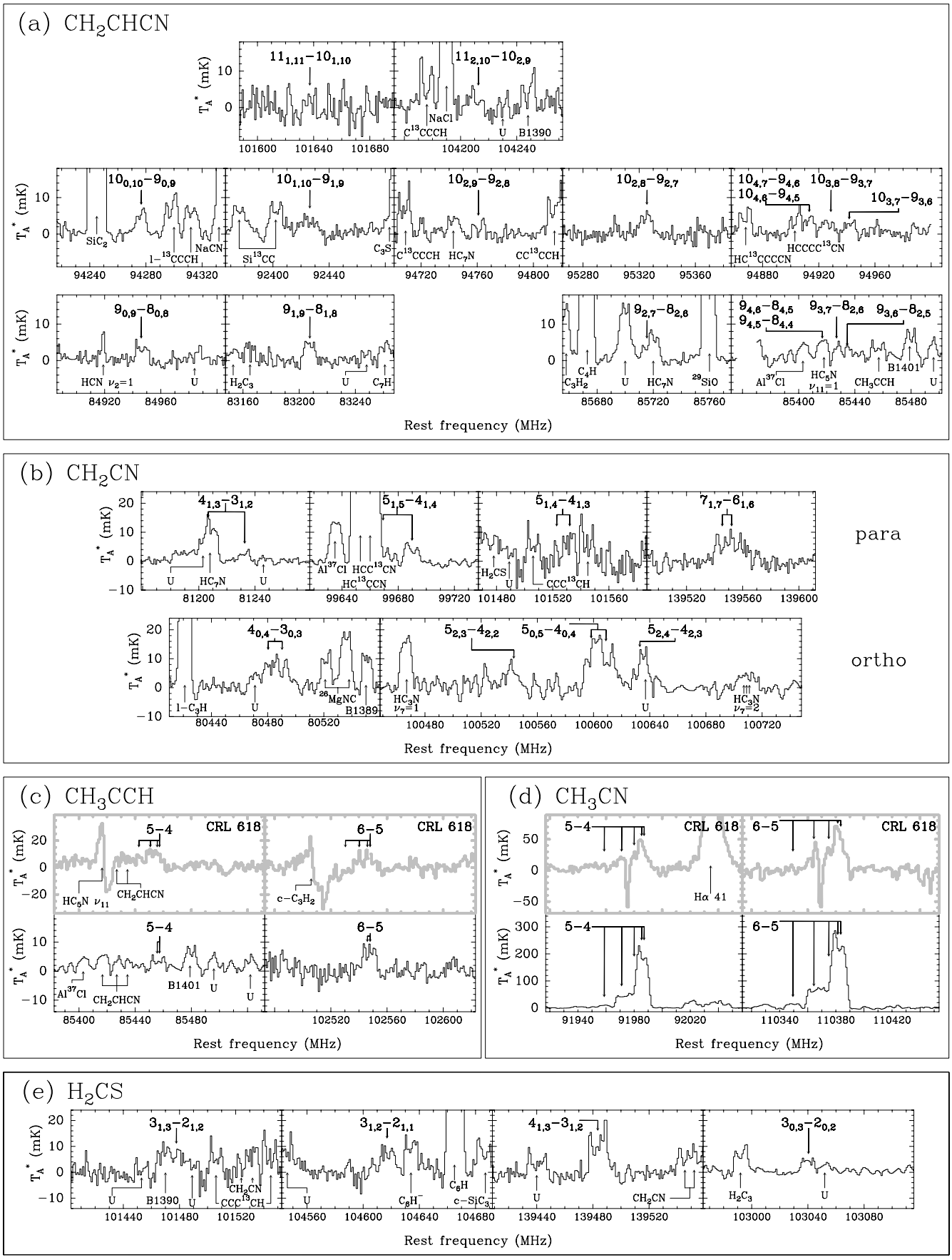

Fig. 1. Rotational lines of **a)** CH_2CHCN, **b)** CH_2CN, **c)** CH_3CCH, **d)** CH_3CN, and **e)** H_2CS observed toward IRC +10216 with the IRAM 30-m telescope at a spectral resolution of 1 MHz. The frequency scale is computed for an LSR source velocity of −26.5 km s^{-1}. For comparison purposes, the thick grey panels show spectra corresponding to CRL 618 (from Pardo et al. 2007). "U" means Unidentified line.

Table 1. Line parameters of CH_2CHCN, CH_2CN, CH_3CCH, and H_2CS in IRC +10216.

Transition	Symmetry	Observed Frequency (MHz)	Calculated Frequency (MHz)	v_{exp} [a] (km s^{-1})	Line Strength	E_{up} (K)	$\int T_A^* dv$ (K km s^{-1})	η_b [b]
			CH_2CHCN					
$9_{0,9}$–$8_{0,8}$		84 946.7(3)	84 946.000	15.5(10)	9.00	20.4	0.11(2)	0.82
$9_{1,9}$–$8_{1,8}$		83 207.5(8)	83 207.505	14.8(10)	8.89	22.1	0.14(2)	0.82
$9_{2,7}$–$8_{2,6}$		85 715.4(5)	85 715.424	14.5[d]	8.56	29.2	0.09(3)[c]	0.82
$9_{3,7}$–$8_{3,6}$		85 427.9(10)	85 426.920	14.5[d]	8.00	40.0	0.09(3)[c]	0.82
$9_{3,6}$–$8_{3,5}$		85 435.6(10)	85 434.526	14.5[d]	8.00	40.0	0.07(2)[c]	0.82
$10_{0,10}$–$9_{0,9}$		94 276.3(10)	94 276.634	14.5[d]	9.99	25.0	0.15(3)	0.81
$10_{1,10}$–$9_{1,9}$		92 426.1(15)	92 426.248	14.5[d]	9.90	26.6	0.11(3)	0.81
$10_{2,9}$–$9_{2,8}$		94 760.9(7)	94 760.781	14.5[d]	9.60	33.7	0.07(2)	0.81
$10_{2,8}$–$9_{2,7}$		95 325.1(8)	95 325.474	14.5[d]	9.60	33.8	0.14(3)	0.81
$10_{3,8}$–$9_{3,7}$		94 926.2(15)	94 928.606	14.5[d]	9.10	44.5	0.09(3)	0.81
$10_{3,7}$–$9_{3,6}$		94 942.0(10)	94 941.630	14.5[d]	9.10	44.5	0.08(2)	0.81
$10_{4,7}$–$9_{4,6}$		94 913.4(10)	94 913.115	14.5[d]	8.40	59.7	0.11(3)[c]	0.81
$10_{4,6}$–$9_{4,5}$			94 913.226		8.40	59.7	[c]	0.81
$11_{1,11}$–$10_{1,10}$		101 637.1(8)	101 637.231	14.5[d]	10.9	31.5	0.07(3)	0.80
$11_{2,10}$–$10_{2,9}$		104 211.5(10)	104 212.646	14.5[d]	10.6	38.7	0.08(3)	0.79
			CH_2CN					
$4_{0,4}$–$3_{0,3}$ $J = 9/2$–$7/2$	O	80 480.5(10)	80 480.384	14.5[d]	4.44	9.7	0.23(6)[c]	0.82
$4_{0,4}$–$3_{0,3}$ $J = 7/2$–$5/2$	O	80 489.6(10)	80 490.261	14.5[d]	3.43	9.7	0.25(6)[c]	0.82
$5_{0,5}$–$4_{0,4}$ $J = 11/2$–$9/2$	O	100 600.2(15)	100 598.383	14.5[d]	5.46	14.5	0.40(7)[c]	0.80
$5_{0,5}$–$4_{0,4}$ $J = 9/2$–$7/2$	O	100 609.6(15)	100 608.832	14.5[d]	4.44	14.5	0.33(6)[c]	0.80
$5_{2,4}$–$4_{2,3}$ $J = 11/2$–$9/2$	O	100 633.2(15)	100 632.957	14.5[d]	4.58	67.2	0.10(3)[c]	0.80
$5_{2,3}$–$4_{2,2}$ $J = 9/2$–$7/2$	O	100 542.5(10)	100 543.214	14.5[d]	3.73	67.2	0.12(3)	0.80
$4_{1,3}$–$3_{1,2}$ $J = 7/2$–$5/2$	P	81 207.6(10)	81 206.601	14.5[d]	3.22	8.9	0.09(3)[c]	0.82
$4_{1,3}$–$3_{1,2}$ $J = 9/2$–$7/2$	P	81 232.4(5)	81 232.654	14.8(5)	4.17	8.9	0.09(2)	0.82
$5_{1,5}$–$4_{1,4}$ $J = 11/2$–$9/2$	P	99 689.5(8)	99 689.833	14.5[d]	5.23	13.4	0.14(4)	0.80
$5_{1,4}$–$4_{1,3}$ $J = 11/2$–$9/2$	P	101 531.6(10)	101 532.055	14.5[d]	5.23	13.7	0.22(6)	0.80
$7_{1,7}$–$6_{1,6}$ $J = 13/2$–$11/2$	P	139 547.1(15)	139 545.477	14.5[d]	6.33	25.9	0.14(4)	0.75
$7_{1,7}$–$6_{1,6}$ $J = 15/2$–$13/2$	P	139 553.4(10)	139 552.138	14.5[d]	7.30	25.9	0.12(4)	0.75
			CH_3CCH					
$J_K = 5_0$–4_0		85 456.4(10)	85 457.299	14.5[d]	5.00	11.5	0.12(4)[c]	0.82
$J_K = 5_1$–4_1			85 455.665		4.80	20.3	[c]	0.82
$J_K = 6_0$–5_0		102 547.5(6)	102 547.983	14.8(6)	6.00	17.2	0.22(5)[c]	0.80
$J_K = 6_1$–5_1			102 546.023		5.83	24.4	[c]	0.80
			H_2CS					
$3_{1,3}$–$2_{1,2}$	O	101 478.1(10)	101 477.750	14.5[d]	2.67	8.1	0.18(4)[c]	0.80
$3_{1,2}$–$2_{1,1}$	O	104 617.5(10)	104 616.969	14.5[d]	2.67	8.4	0.23(3)	0.79
$4_{1,3}$–$3_{1,2}$	O	139 483.8(5)	139 483.422	14.1(6)	3.75	15.1	0.36(5)	0.75
$3_{0,3}$–$2_{0,2}$	P	103 040.3(5)	103 040.396	14.6(7)	3.00	9.9	0.13(2)	0.80

Note. The numbers in parentheses are errors in units of the last digits; the 1σ error in $\int T_A^* dv$ is derived from least-squares fits and does not include the calibration uncertainty of 10%. [a] v_{exp} stands for expansion velocity and is computed as half the full linewidth at zero level. [b] η_b is B_{eff}/F_{eff}, i.e. the ratio of T_A^* to T_{mb}. A superscript "*c*" denotes a partly blended line while "*d*" indicates that the linewidth parameter v_{exp} has been fixed to 14.5 km s^{-1}. The calculated frequencies of CH_2CN correspond to the strongest hyperfine component, as measured by Ozeki et al. (2004). CH_2CN and H_2CS lines have ortho (O) or para (P) symmetry; E_{up} is the energy of the upper level of the transition above the O or P ground state.

different in these two objects. In IRC +10216 both molecules are present with a similar abundance (CH_3CCH/CH_3CN = 0.6). In contrast, in CRL 618 methylacetylene is much more abundant than methyl cyanide (Pardo et al. 2007), not only in the region corresponding to the first post-AGB ejections (CH_3CCH/CH_3CN = 6) but also in the warm and dense inner regions where UV photons efficiently drive a rich C-based photochemistry (CH_3CCH/CH_3CN = 15). Such a stage has not yet been reached by IRC +10216.

The four lines of H_2CS observed in IRC +10216 have similar E_{up} values, thus it is rather difficult to constrain the rotational temperature. Assuming an statistical O/P ratio of 3:1 and a rotational temperature of 30 K we derive a total column density $N_{tot} = 1.0 \times 10^{13}$ cm^{-2} for thioformaldehyde, which is almost twice larger than that of formaldehyde (Ford et al. 2004; see Table 2).

4. Chemical modelling

In order to explain how the detected species are formed we have constructed a detailed chemical model of the outer envelope. The chemical network consists of 385 gas phase species linked by 6547 reactions, whose rate constants have been taken from Cernicharo (2004), Agúndez & Cernicharo (2006) and from the UMIST Database for Astrochemistry (Woodall et al. 2007). The temperature and density radial profiles as well as other physical assumptions are taken from Agúndez & Cernicharo (2006). The resulting abundance radial profiles for CH_2CHCN, CH_2CN,

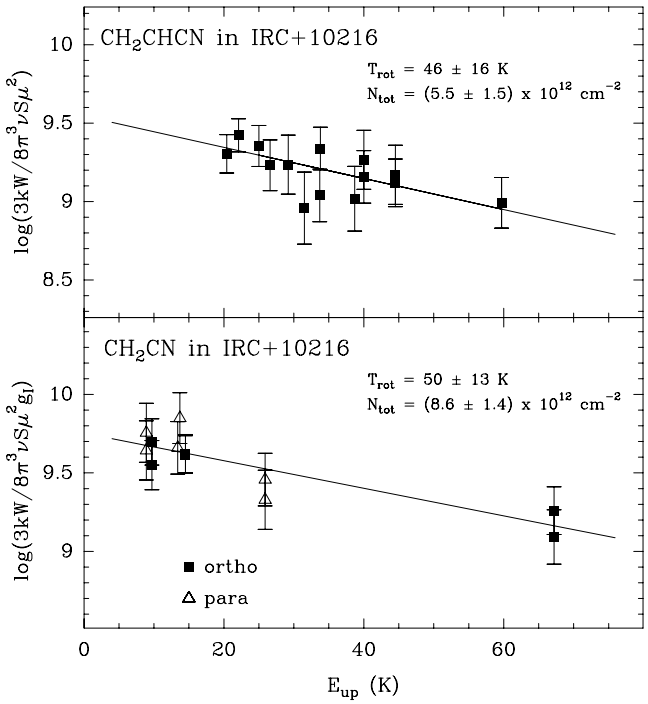

Fig. 2. Rotational temperature diagrams of CH_2CHCN and CH_2CN in IRC +10216. T_{rot} and N_{tot} have been determined from a weighted least-squares fit to the observational points, and their uncertainties reflect the 1σ errors in the fits to the line profiles plus the 10% estimated uncertainty in the calibration.

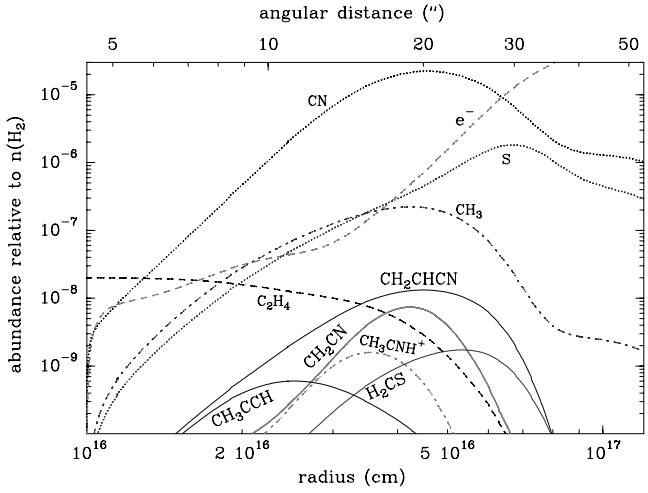

Fig. 3. Abundances of CH_2CHCN, CH_2CN, CH_3CCH, H_2CS (solid lines) and related species (dotted and dashed lines) given by the chemical model, as a function of radius (*bottom axis*) and angular distance (*top axis*) for an assumed stellar distance of 150 pc.

CH_3CCH, H_2CS and related species are plotted in Fig. 3. The model predicts that these four molecules would display an extended shell-type distribution with an angular radius of about 20″. The predicted and observed column densities are summarized in Table 2.

Vinyl cyanide results from the reaction between CN and ethylene, the latter being found in the inner envelope with an abundance relative to H_2 of 2×10^{-8} (Goldhaber et al. 1987). This reaction has been studied in the laboratory and found to be very rapid at low temperature (Sims et al. 1993) yielding vinyl cyanide (Choi et al. 2004):

$$CN + C_2H_4 \longrightarrow CH_2CHCN + H. \quad (1)$$

Our model predicts a total column density $N_{tot} = 1.4 \times 10^{13}$ cm^{-2}, which reasonably agrees with the value derived from the observations[2]. The analogue of reaction (1) replacing C_2H_4 by C_2H_2 is the main formation pathway of HC_3N in IRC +10216. The much larger column density of HC_3N compared to that of CH_2CHCN (more than two orders of magnitude; see Table 2) reflects the large excess of acetylene over ethylene in the inner envelope of IRC +10216. In dark clouds, reaction (1) is also probably the main formation route to vinyl cyanide (Herbst & Leung 1990).

The dissociative recombination (DR) of the ion CH_3CNH^+ is the major pathway to form both CH_2CN and CH_3CN:

$$CH^+ \xrightarrow{H_2} CH_2^+ \xrightarrow{H_2} CH_3^+ \xrightarrow{HCN} CH_3CNH^+ \begin{array}{l} \xrightarrow{e^-} CH_2CN \\ \xrightarrow{e^-} CH_3CN. \end{array} \quad (2)$$

The branching ratios of the channels giving CH_2CN and CH_3CN are not known and are assumed to be equal. In our model, the major destruction process for both CH_2CN and CH_3CN is the photodissociation by interstellar UV photons. The photodissociation rate of CH_3CN has been calculated by Roberge et al. (1991) but that of CH_2CN is unknown and we assume it to be the same as that of CH_3CN. Since the chemistry of these two molecules is relatively well constrained in IRC +10216, they are formed by the same reaction and their destruction is dominated by just one process, we may use the observed CH_2CN/CH_3CN ratio to estimate the branching ratios of the DR of the CH_3CNH^+ ion. We find an 80% for the channel (CH_3CN + H) and 20% for (CH_2CN + H_2 or 2H). This estimate will be strongly affected if the photodissociation rate of CH_2CN is very different from that of CH_3CN but not if, as suggested by Herbst & Leung (1990) and Turner et al. (1990), CH_2CN reacts with atomic oxygen, the abundance of which is low in IRC +10216 at the radius where CH_2CN is present.

The related species CH_3C_3N is formed by the same sequence of reactions that produces CH_3CN, just replacing HCN by HC_3N. Its predicted column density is lower than that of

Table 2. Column densities of selected molecules in IRC +10216.

Molecule	T_{rot} (K)	N_{tot} (cm^{-2})		
		observed	calculated	
			This work	[1]
HC_3N	15	2.2(15)[2]	2.8(15)	3.6(15)
CH_2CHCN	46	5.5(12)	1.4(13)	2.2(11)
CH_2CN	50	8.6(12)	4.6(12)	1.4(13)
CH_3CN	40	3.0(13)[2]	6.3(12)	6.8(12)
CH_3C_3N	30[a]	<1.3(12)[2]	1.2(11)	1.4(12)
CH_3CCH	30[a]	1.8(13)	1.1(12)	8.0(12)
CH_3C_4H	30[a]	<9.7(12)[2]	8.2(12)	9.0(12)
H_2CO	28	5.4(12)[3]	2.8(12)	–
H_2CS	30[a]	1.0(13)	1.3(12)	4.4(11)

Note. $a(b)$ refers to $a \times 10^b$. A superscript "a" indicates an assumed rotational temperature.
References. [1]: Millar et al. (2000); [2]: from unpublished IRAM 30-m data; [3]: from the observations by Ford et al. (2004).

[2] The radial column densities given by the chemical model are multiplied by a factor 2 to get the total column densities across the envelope N_{tot}.

CH_3CN by more than one order of magnitude. However, since our model predicts less CH_3CN than observed, the CH_3^+ ion is probably underproduced, the column density of CH_3C_3N is most likely underestimated. If CH_3C_3N were present with a column density of several 10^{11} cm^{-2}, the expected brightness temperatures would be a few mK and therefore it could be detectable. In fact, our IRAM 30-m line survey at λ 3 mm of IRC +10216 (Cernicharo et al., in preparation) shows two unidentified features with T_A^* ~2−3 mK at 86 756 MHz and 103 280 MHz that could correspond to the $J = 21-20$ and $J = 25-24$ transitions of CH_3C_3N respectively. The spectra covering other 3 mm transitions of CH_3C_3N are not sensitive enough to confirm or discard the presence of this species.

The synthesis of CH_3CCH involves various ion-molecule reactions with the dissociative recombination of the ions $C_3H_5^+$ and $C_4H_5^+$ as the last step. The model underestimates the observed CH_3CCH column density by one order of magnitude, probably due to uncertainties and/or incompleteness in the chemical network. The heavier chain CH_3C_4H is predicted to have a column density even higher than that of CH_3CCH. The smaller rotational constant B and larger rotational partition function of CH_3C_4H makes it less favorable for being observed at millimetre wavelengths. However its larger dipole moment ($\mu_{CH_3C_4H} = 1.207$ D versus $\mu_{CH_3CCH} = 0.784$ D) could result in line intensities similar to those of CH_3CCH. Our IRAM 30-m λ 3 mm data shows an unidentified feature with $T_A^* \sim 3$ mK at 81 427 MHz that could be assigned to the $J = 20-19$ transition of CH_3C_4H. As occurs with CH_3C_3N, the detection of CH_3C_4H remains tentative since our current spectra covering other 3 mm lines is not sensitive enough.

Lastly, as previously discussed by Agúndez & Cernicharo (2006), H_2CS is formed by the neutral-neutral reaction S + CH_3 and the dissociative recombination of H_3CS^+. The predicted column density is $N_{tot} = 1.3 \times 10^{12}$ cm^{-2}, which is a factor 7 lower than the value derived from observations. We note that a significant fraction of both H_2CO and H_2CS could be formed on grain surfaces by hydrogenation of CO and CS respectively. It is remarkable that in IRC +10216 thioformaldehyde is more abundant than formaldehyde, despite the cosmic abundance of oxygen being 50 times larger than that of sulphur. The carbon-rich character of the CSE makes oxygen-bearing species to have a very low abundance.

5. Excitation mechanism: infrared pumping

The chemical model predicts that the molecules formed in the outer envelope have their peak abundances between 3×10^{16} cm and 6×10^{16} cm, which corresponds to angular radii of 13″−26″ for an assumed distance to IRC +10216 of 150 pc (see Fig. 3). Interferometric observations at millimetre wavelengths have located the molecular shell at about 15″ (Guélin et al. 1993; Audinos et al. 1994; Lucas et al. 1995) although the exact value depends on the molecule and transition mapped. At this distance the gas density is a few 10^4 cm^{-3} and the gas kinetic temperature is lower than 20 K (Skinner et al. 1999). We may ask ourselves how the rotational levels are excited to result in rotational temperatures for CH_2CHCN and CH_2CN of 40−50 K, well above the gas kinetic temperature.

Collisions with H_2 molecules do not seem to be responsible of such an excitation. For example, in the case of the cyanomethyl radical the collision coefficients γ_{ul} for CH_2CN-H_2 have not been measured or calculated but should be similar to those calculated for CH_3CN-H_2 by Green (1986), at least for the $K_a = 0$ ladder (see Turner et al. 1990, for more details). Thus, adopting a deexcitation collision coefficient $\gamma_{ul} = 10^{-10}$ cm^3 s^{-1}, typical for $\Delta J = -1$, $\Delta K = 0$ transitions of CH_3CN, and an Einstein coefficient for spontaneous emission of $A_{ul} = 5 \times 10^{-5}$ s^{-1}, the resulting critical density is $n_{crit} = A_{ul}/\gamma_{ul} = 5 \times 10^5$ cm^{-3}. This value is larger than the gas density expected at a distance of $4-5 \times 10^{16}$ cm, so that the rotational levels are not thermalized and collisional excitation by itself should result in a rotational temperature lower than the gas kinetic temperature. In the cases of molecules such as CH_2CN, with a relatively large dipole moment, i.e. whose rotational levels are hardly thermalized in the outer envelope, and which have rotational temperatures above the kinetic temperature of the gas, the excitation is most probably dominated by a radiative mechanism.

Absorption of infrared photons and pumping into excited vibrational levels followed by radiative decay to rotational levels in the ground vibrational state has been invoked many years ago as the main excitation mechanism for some circumstellar molecules in IRC +10216 (Morris 1975). As a matter of fact, several molecules present in the outer envelope have been detected in excited vibrational states, e.g. C_4H $v_7 = 1$, 2 ($v_7 = 131$ cm^{-1}; Guélin et al. 1987; Yamamoto et al. 1987), HC_3N $v_7 = 1$ ($v_7 = 223$ cm^{-1}; Cernicharo et al. 2000), l-C_3H $v_4 = 1$ ($v_4 = 28$ cm^{-1}; Cernicharo et al. 2000), and SiC_2 $v_3 = 1$ ($v_3 = 160$ cm^{-1}; Gensheimer & Snyder 1997; Cernicharo et al. 2000). Radiative transfer calculations have also evidenced the importance of infrared pumping in exciting molecules such as HC_5N (Deguchi & Uyemura 1984) and H_2O (Agúndez & Cernicharo 2006) in IRC +10216. For this process to be efficient, the molecules must have vibrational modes active in the infrared, sufficiently strong and with a frequency at which the central object emits a high flux. The spectrum of IRC +10216 as seen by ISO peaks at a wavelength of ~10 μm (Cernicharo et al. 1999) and the flux is very large within a wide wavelength range (see below). In fact, the excited vibrational states of C_4H, HC_3N, l-C_3H, and SiC_2 detected have wavelengths between 45 and 357 μm.

In the case of CH_2CHCN, there exists a large number of vibrational modes, the strongest of which are the bending modes ν_{12} and ν_{13} at 972 cm^{-1} (10.3 μm) and 954 cm^{-1} (10.5 μm) respectively (Cerceau et al. 1985; Khlifi et al. 1999). For CH_2CN the only available experimental information concerns the ν_5 mode at 664 cm^{-1} (15.1 μm; Sumiyoshi et al. 1996).

In order to give a quantitative estimate of how important is the infrared pumping compared to excitation by collisions, we may evaluate the rates of both processes. The excitation by infrared pumping operates through absorption of an infrared photon and promotion of a molecule from a given rotational level in the ground vibrational state (v_0, J'') to another rotational level in an excited vibrational state (v_1, J), from which it decays spontaneously to a different rotational level of the ground vibrational state (v_0, J') through either a single transition or a radiative cascade process. The rate at which the latter level (v_0, J') is populated is then governed by the rate of the absorption process: v_0, $J'' \rightarrow v_1$, J, which is given by:

$$R_{\rightarrow v_0,J'} = B_{v_0 \rightarrow v_1} 4\pi \overline{J} \qquad [=] \quad \mathrm{s}^{-1} \tag{3}$$

where $B_{v_0 \rightarrow v_1}$ is the Einstein coefficient for absorption and $\overline{J}$ is the mean intensity, averaged over all solid angles, at the frequency of the infrared band. The deexcitation from the level (v_1, J) can be assumed as instantaneous in IRC +10216 for all relevant wavelengths.

The rate at which the rotational level (v_0, J') is populated by collisions with H_2 molecules is given by:

$$C_{\rightarrow v_0,J'} = \gamma_{lu} n(H_2) \qquad [=] \quad \mathrm{s}^{-1} \tag{4}$$

where γ_{lu} is the coefficient for rotational excitation, within the ground vibrational state, by collisions with H_2 and $n(H_2)$ is the H_2 volume density.

To estimate the infrared flux in the outer envelope we have used the radiative transfer model described in Fonfría et al. (2007) and the ISO observations of IRC +10216 (Cernicharo et al. 1999). The best fit to the observed continuum between 7 and 27 μ is shown in the lower panel of Fig. 4. The SiC band at 11.3 μm is correctly reproduced. At long wavelengths the model seems to underestimate the absolute observed flux, which is nevertheless affected by the uncertainties in the multiplicative calibration factors applied in the data reduction (Swinyard et al. 1998).

The model has been used to calculate the radiation field at a distance of $r = 5 \times 10^{16}$ cm (20″) from the star (see upper panel in Fig. 4). The calculated spectral energy distribution can be approximated by a blackbody with a radius $R_{bb} = 13\ R_*$ and a temperature $T_{bb} = 550$ K (see upper panel in Fig. 4), so that we may use the Planck function for such a blackbody to evaluate $4\pi\overline{J}$ and see whether the rate for infrared pumping exceeds or not the collisional excitation rate. The radiative over collisional "excess" ($R_{\rightarrow v_0,J'}/C_{\rightarrow v_0,J'}$) may be evaluated as:

$$\frac{R_{\rightarrow v_0,J'}}{C_{\rightarrow v_0,J'}} = \frac{(g_{v_1,J}/g_{v_0,J''})A_{v_1\rightarrow v_0}(R_{bb}/r)^2}{4[e^{(h\nu_{IR}/kT_{bb})} - 1]\gamma_{lu}n(H_2)} \quad (5)$$

where $(g_{v_1,J}/g_{v_0,J''})$ is the ratio between the statistical weights of the (v_1, J) and (v_0, J'') states, ν_{IR} and $A_{v_1\rightarrow v_0}$ are the frequency and Einstein coefficient of spontaneous emission of the vibrational transition, and h and k are the Planck and Boltzmann constants. Adopting, to a first approximation, $(g_{v_1,J}/g_{v_0,J''})$ equal to unity and taking into account the variation of the H_2 volume density with radius, $n(H_2)$ [cm^{-3}] $= 3.1 \times 10^{37}/r^2$ with r expressed in cm (see e.g. Agúndez & Cernicharo 2006), we arrive at:

$$\frac{R_{\rightarrow v_0,J'}}{C_{\rightarrow v_0,J'}} = \frac{5.8 \times 10^{-9} A_{v_1\rightarrow v_0}[s^{-1}]}{\{e^{(26.2/\lambda_{IR}[\mu m])} - 1\}\gamma_{lu}[cm^3\ s^{-1}]}\ . \quad (6)$$

The radiative over collisional excess is independent of radius, since both the radiation field and the H_2 volume density decrease with the square of the radius, and only depends on the wavelength and strength of the vibrational band and on the collision coefficient. Just as an example, if we take typical values $\gamma_{lu} = 10^{-10}$ cm^3 s^{-1} and $A_{v_1\rightarrow v_0} = 1$ s^{-1} (adequate for vibrational modes sufficiently strong), we obtain that the rate of infrared pumping exceeds the collisional excitation rate for vibrational modes with wavelengths λ_{IR} larger than ~6 μm. Bending modes have usually wavelengths larger than this lower limit, thus if the mode is active in the infrared and sufficiently strong, the rotational levels of that molecule will be mostly excited through infrared pumping in the circumstellar envelope of IRC +10216. For example, the two bending modes of CH_2CHCN ν_{12} (972 cm^{-1}; 10.3 μm) and ν_{13} (954 cm^{-1}; 10.5 μm) have Einstein coefficients for spontaneous emission of 2.9 s^{-1} and 2.8 s^{-1} respectively[3]. The collision coefficients γ_{ul} for CH_2CHCN-H_2 are not known, but according to Eq. (6), values as large as 5×10^{-9} cm^3 s^{-1} are required for making collisions to dominate over infrared pumping. Thus, this molecule will be preferably excited by infrared pumping through these two bending modes in IRC +10216.

6. Discussion

The detection in IRC +10216 of the partially saturated organic molecules reported in this Paper invites for a comparison to TMC-1, the other Galactic source that displays, together with IRC +10216, the largest wealth in unsaturated carbon chain molecules. For that purpose we have represented in Fig. 5 the fractional abundances of carbon chains in these two sources as a function of the number of heavy atoms.

Chemistry proceeds in a different way in these two objects. In IRC +10216 interstellar UV photons drive the chemistry by photodissociating the closed shell molecules flowing out from the inner envelope. In TMC-1 the gas is well shielded against the interstellar UV field and the built-up of molecules is driven by ionisation by cosmic rays. This introduces a sharp difference in the time scales of the processes being at work. In IRC +10216 the gas travels throughout the CSE during a few thousands of years and the chemical processes take place in shorter time scales. In TMC-1 the built-up of molecules has time scales of the order of millions of years and the depletion from the gas of some species, due to condensation on grains, is a major issue at late times. A consequence of this is the lower level at which molecules are present in TMC-1 compared to IRC +10216. As an example we see in Fig. 5 that the most abundant carbon chains in both sources are those with a highly unsaturated character, cyanopolyynes and polyyne radicals, the abundances of which are larger in IRC +10216 than in TMC-1 by more than one order of magnitude.

Another important difference between these two sources could lie in the C/O ratio. In IRC +10216, the processes of dredge-up related to the AGB phase have resulted in a photospheric C/O ratio higher than 1. This controls the chemistry in

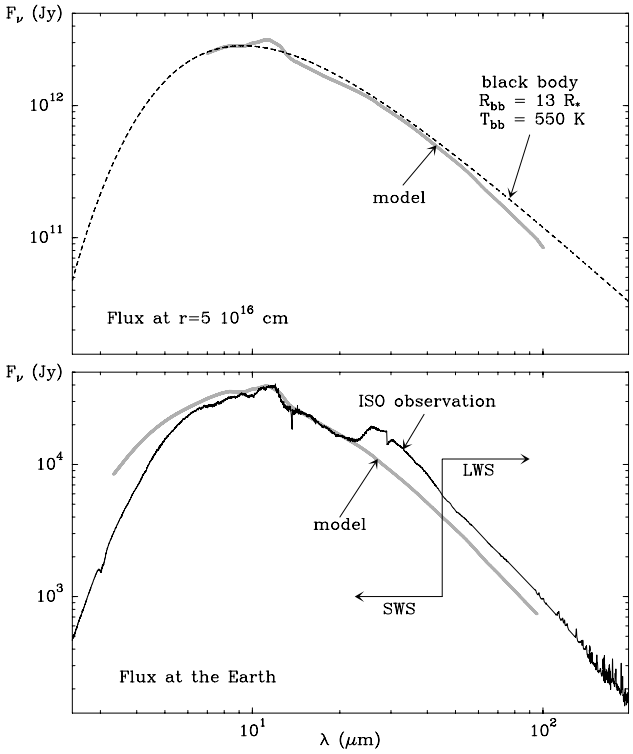

Fig. 4. Spectral energy distribution of IRC +10216 at infrared wavelengths. The lower panel shows the fit to the continuum observed by ISO. Most of the discrepancies between model and observations in the 7−20 μm range are likely due to molecular infrared bands, which are not considered in the model. In the top panel the radiation field ($4\pi\overline{J}$) at a point 5×10^{16} cm away from the star, as given by the model, is compared to that expected with a central blackbody of radius 13 R_* and temperature of 550 K.

[3] See e.g. http://www.lesia.obspm.fr/crovisier/basemole/

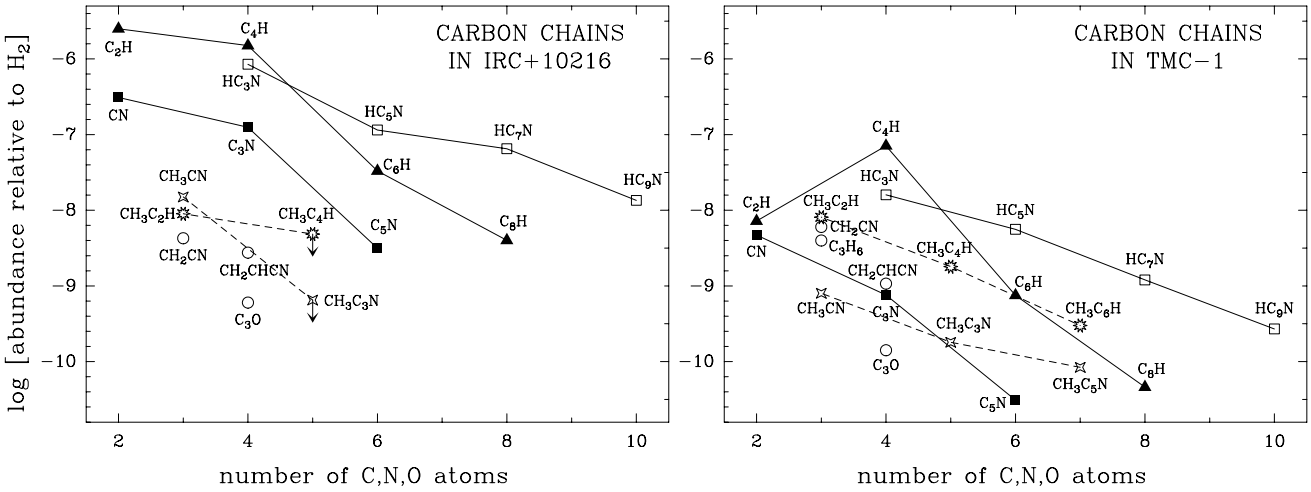

Fig. 5. Abundances of carbon chain molecules in IRC +10216 and TMC-1. The diagram is an extension of that published by Cernicharo et al. (1987). The fractional abundances relative to H_2 are computed from the molecular column densities and the total H_2 column density. We use $N(H_2) = 10^{22}$ cm^{-2} in TMC-1 (Cernicharo & Guélin 1987) and $N(H_2) = 2 \times 10^{21}$ cm^{-2} in IRC +10216. The latter value corresponds to the total H_2 column density contained in an outer shell extending from 2×10^{16} cm to 7×10^{16} cm, where all the molecules considered in the diagram are most probably present. The choice of these boundaries is not critical for the values of the molecular abundances. Only if any of the molecules considered does not form in the outer envelope but in the inner regions of the CSE, then its abundance would be substantially overestimated.

the outer envelope: almost all the oxygen keeps locked into CO during most of the expansion while the carbon in excess can participate in a rich carbon chemistry. In TMC-1 it is not clear whether the C/O ratio is higher or lower than 1. The large number of carbon chains found argues in favor of a C/O ratio >1, which is unusual for a dense cloud, and some chemical models have used it because a better agreement with observations is achieved (Smith et al. 2004). On the other hand, oxygen is cosmically more abundant than carbon and TMC-1 contains a substantial number of O-bearing molecules (Ohishi & Kaifu 1998), which points toward a C/O ratio <1. If the latter is true, then the carbon chemistry would be limited due to the presence of atomic oxygen which tends to destroy the chemical complexity (Herbst et al. 1994), something that does not happen in IRC +10216 due to the unavailability of free atomic oxygen (Millar & Herbst 1994). This could also explain the systematically lower abundances of carbon chains in TMC-1 compared to IRC +10216.

If we focus on partially saturated species, such as methylpolyynes, methylcyanopolyynes, CH_2CN or CH_2CHCN, then we note that in IRC +10216 they are present at a lower level than the highly unsaturated species, while in TMC-1 partially saturated and highly unsaturated molecules have abundances in many cases comparable; e.g. compare the ratio of the abundances of CH_2CN and HC_3N in both sources. Thus, chemistry seems to favor the presence of species with a higher degree of saturation in dark clouds than in C-rich circumstellar envelopes. The recent detection of the highly saturated hydrocarbon propylene in TMC-1 (Marcelino et al. 2007) supports this point.

In IRC +10216 the UV field which drives the chemistry is mostly photodissociating but not ionising, so that the dominant reactions are neutral-neutral rather than ion-molecule. In TMC-1, the chemistry is triggered by cosmic rays ionisation, and ion-molecule reactions do greatly participate in the built-up of molecules. Note that chemical models have traditionally explained the formation of molecules in interstellar clouds by means of ion-molecule reactions. However, since it was discovered that some neutral-neutral reactions are very rapid at low temperatures, it is now thought that these latter reactions dominate the formation of highly unsaturated carbon chains such as cyanopolyynes (Herbst et al. 1994). That is, in general terms we may state that "current gas phase chemical models form highly unsaturated carbon chains mostly by neutral-neutral reactions while partially saturated molecules are generally formed by ion-molecule reactions". Therefore, ion-molecule reactions could be, ultimately, the responsible of the higher degree of saturation observed in TMC-1 compared to IRC +10216. Grain surface reactions, which are very efficient in producing highly saturated molecules, could also play a role in the peculiar chemistry of TMC-1. However, it is not clear how these mantle species would be desorbed to the gas phase at the low temperatures prevailing in these regions.

7. Conclusions

In summary, we have shown that apart from the abundant highly unsaturated cyanopolyynes and polyyne radicals, analogous molecules with a higher degree of saturation are also present in IRC +10216. In this paper we have presented the detection of CH_2CHCN, CH_2CN, CH_3CCH, and also of thioformaldehyde. The relatively high rotational temperatures, 40−50 K, derived for CH_2CHCN and CH_2CN suggest that these species are excited in the circumstellar envelope through radiative pumping to excited vibrational states.

The formation of partially saturated organic molecules in IRC +10216 resembles that occurring in cold dense clouds and stresses the similarity between the chemistry in these two types of sources. However, unlike in TMC-1, their abundances are much lower than those of highly unsaturated molecules, like cyanopolyynes and polyyne radicals, which reflects the differences in the chemical processes at work in dark clouds and C-rich circumstellar envelopes.

Acknowledgements. We acknowledge comments and suggestions from the referee. This work has been supported by Spanish MEC through grants AYA2003-2785, ESP2004-665 and AYA2006-14876, by "Comunidad de Madrid" under PRICIT project S-0505/ESP-0237 (ASTROCAM) and by the European Community's human potential Programme under contract MCRTN-CT-2004-51230 (The Molecular Universe). MA also acknowledges funding support from Spanish MEC through grant AP2003-4619.

References

Agúndez, M., & Cernicharo, J. 2006, ApJ, 650, 374
Audinos, P., Kahane, C., & Lucas, R. 1994, A&A, 287, L5
Broten, N. W., MacLeod, J. M., Avery, L. W., et al. 1984, ApJ, 276, L25
Burrell, P. M., Bjarnov, E., & Schwendeman, R. H. 1980, J. Mol. Spectr., 82, 193
Cerceau, F., Raulin, F., Courtin, R., & Gautier, D. 1985, Icarus, 62, 207
Cernicharo, J. 2004, ApJ, 608, L41
Cernicharo, J., & Guélin, M. 1987, A&A, 176, 299
Cernicharo, J., Guélin, M., Menten, K. M., & Walmsley, C. M. 1987, A&A, 181, L1
Cernicharo, J., Yamamura, I., González-Alfonso, E., et al. 1999, ApJ, 526, L41
Cernicharo, J., Guélin, M., & Kahane, C. 2000, A&AS, 142, 181
Cernicharo, J., Heras, A. M., Pardo, J. R., et al. 2001, ApJ, 546, L127
Choi, N., Blitz, M. A., McKee, K., et al. 2004, Chem. Phys. Lett., 384, 68
Deguchi, S., & Uyemura, M. 1984, ApJ, 285, 153
Fabricant, B., Krieger, D., & Muenter, J. S. 1977, J. Chem. Phys., 67, 1576
Fonfría, J. P., Cernicharo, J., Richter, M. J., & Lacy, J. 2007, ApJ, 673, 445
Ford, K. E. S., Neufeld, D. A., Schilke, P., & Melnick, G. J. 2004, ApJ, 614, 990
Gardner, F. F., & Winnewisser, G. 1975, ApJ, 195, L127
Gensheimer, P. D., & Snyder, L. E. 1997, ApJ, 490, 819
Goldhaber, D. M., Betz, A. L., & Ottusch, J. J. 1987, ApJ, 314, 356
Green, S. 1986, ApJ, 309, 331
Guélin, M., Cernicharo, J., Navarro, S., et al. 1987, A&A, 182, L37
Guélin, M., Lucas, R., & Cernicharo, J. 1993, A&A, 280, L19
Herbst, E., & Leung, C. M. 1990, A&A, 233, 177
Herbst, E., Lee, H.-H., Howe, D. A., & Millar, T. J. 1994, MNRAS, 268, 335
Khlifi, M., Nollet, M., Paillous, P., et al. 1999, J. Mol. Spectr., 194, 206
Irvine, W. M., Höglund, B., Friberg, P., et al. 1981, ApJ, 248, L113
Irvine, W. M., Friberg, P., Hjalmarson, Å., et al. 1988, ApJ, 334, L107
Johansson, L. E. B., Andersson, C., Elldér, J., et al. 1984, A&A, 130, 227
Lafont, S., Lucas, R., & Omont, A. 1982, A&A, 106, 201
Lovas, F. J., Remijan, A. J., Hollis, J. M., et al. 2006, ApJ, 637, L37
Lucas, R., Guélin, M., Kahane, C., et al. 1995, Ap&SS, 224, 293
Marcelino, N., Cernicharo, J., Agúndez, M., et al. 2007, ApJ, 665, L127
Matthews, H. E., & Sears, T. J. 1983a, ApJ, 267, L53
Matthews, H. E., & Sears, T. J. 1983b, ApJ, 272, 149
Millar, T. J., & Herbst, E. 1994, A&A, 288, 561
Millar, T. J., Herbst, E., & Bettens, R. P. A. 2000, MNRAS, 316, 195
Morris, M. 1975, ApJ, 197, 603
Müller, H. S. P., Pracna, P., & Horneman, V.-M. 2002, J. Mol. Spectr., 216, 397
Müller, H. S. P., Schlöder, F., Stutzki, J., & Winnewisser, G. 2005, J. Mol. Struct., 742, 215
Nejad, L. A. M., & Millar, T. J. 1987, A&A, 183, 279
Ohishi, M., & Kaifu, N. 1998, Faraday Discuss., 109, 205
Ozeki, H., Hirao, T., Saito., S., & Yamamoto, S. 2004, ApJ, 617, 680
Pardo, J. R., & Cernicharo, J. 2006, ApJ, 654, 978
Pardo, J. R., Cernicharo, J., Goicoechea, J. R., et al. 2007, ApJ, 661, 250
Pickett, H. M., Poynter, R. L., Cohen, E. A., et al. 1998, J. Quant. Spec. Radiat. Transf., 60, 883
Roberge, W. G., Jones, D., Lepp, S., & Dalgarno, A. 1991, ApJS, 77, 287
Sims, I. R., Queffelec, J.-L., Travers, D., et al. 1993, Chem. Phys. Lett., 211, 461
Sinclair, M. W., Fourikis, N., Ribes, J. C., et al. 1973, Aust. J. Phys., 26, 85
Skinner, C. J., Justtanont, K., Tielens, A. G. G. M., et al. 1999, MNRAS, 302, 293
Smith, I. W. M., Hersbt, E., & Chang, Q. 2004, MNRAS, 350, 323
Snyder, L. E., & Buhl, D. 1973, Nature Phys. Sci., 243, 45
Snyder, L. E., Hollis, J. M., Jewell, P. R., et al. 2006, ApJ, 647, 412
Stolze, M., & Sutter, D. H. 1985, Z. Naturforsch. A, 40, 998
Sumiyoshi, Y., Tanaka, K., & Tanaka, T. 1996, J. Chem. Phys., 104, 1839
Swinyard, B. M., Burgdorf, M. J., Clegg, P. E., et al. 1998, Proc. SPIE, 3354, 888
Trambarulo, R., & Gordy, W. 1950, J. Chem. Phys., 18, 1613
Turner, B. E., Friberg, P., Irvine, W. M., et al. 1990, ApJ, 355, 546
Walmsley, C. M., Jewell, P. R., Snyder, L. E., & Winnewisser, G. 1984, A&A, 134, L11
Woodall, J., Agúndez, M., Markwick-Kemper, A. J., & Millar, T. J. 2007, A&A, 466, 1197
Yamamoto, S., Saito, S., Guélin, M., et al. 1987, ApJ, 323, L149